Local Versus Global Two-Photon Interference in Quantum Networks

Thomas Nitsche,[1] Syamsundar De,[1,*] Sonja Barkhofen,[1] Evan Meyer-Scott,[1] Johannes Tiedau,[1] Jan Sperling,[1] Aurél Gábris,[2,3] Igor Jex,[2] and Christine Silberhorn[1]

[1]*Applied Physics, Paderborn University, Warburger Straße 100, 33098 Paderborn, Germany*

[2]*Department of Physics, Faculty of Nuclear Sciences and Physical Engineering, Czech Technical University in Prague, Břehová 7, 115 19 Praha 1–Staré Město, Czech Republic*

[3]*Wigner Research Centre for Physics, Konkoly-Thege M. út 29–33, H-1121 Budapest, Hungary*

(Received 15 May 2020; accepted 27 October 2020; published 20 November 2020)

We devise an approach to characterizing the intricate interplay between classical and quantum interference of two-photon states in a network, which comprises multiple time-bin modes. By controlling the phases of delocalized single photons, we manipulate the global mode structure, resulting in distinct two-photon interference phenomena for time-bin resolved (local) and time-bucket (global) coincidence detection. This coherent control over the photons' mode structure allows for synthesizing two-photon interference patterns, where local measurements yield standard Hong-Ou-Mandel dips while the global two-photon visibility is governed by the overlap of the delocalized single-photon states. Thus, our experiment introduces a method for engineering distributed quantum interferences in networks.

DOI: 10.1103/PhysRevLett.125.213604

Introduction.—The naive idea that our world consists of particles, reminiscent of tiny billiard balls, which govern the laws of physics has been refuted. Rather, it is waves, be it classical or quantum, which describe nature best—covering areas ranging from gravity to hydrodynamics to optics to subatomic systems. For example, quantum field theories merely consider elementary particles as excitations of an underlying quantum field, such as photons for light [1]. Thus, even particles must be able to interfere, which was demonstrated, e.g., in pioneering double-slit experiments with electrons [2]. To speak of genuine quantum interference, we must consider at least two particles, like in the seminal Hong-Ou-Mandel (HOM) effect in the interference of two photons [3]. With recent theoretical and technological advances in the control of quantum systems, there is a spur of interest in how such multiparticle interferences can manifest themselves in large networks [4–10].

The control of classical coherence properties and its utilization is ubiquitous in multichannel optical systems [11], which rely on different interfering pathways. Examples include coherent control in spectroscopy, chemistry, and various imaging systems. The strong demand for developing efficient coherent control strategies for large quantum systems arose from innovations in quantum information processing and technologies that exploit quantum coherence to its full extent [12–14].

Photonic networks provide an excellent platform for studying large-scale coherence effects under designed conditions [15]. For both practical and fundamental purposes, the quality of a network—benchmarked by stability, scalability, and reconfigurability—mainly depends on its coherence and control properties. Networks allow for a natural distinction of local and global features, and the introduction of multiple quantum particles to passive networks is key to many quantum communication schemes [13]. Earlier studies aimed at manipulating coherence of photons to alter the fundamental HOM effect [16], exposing an intricate connection of classical and quantum interference [17–20]. This further inspired many studies of passive multiphoton interferences dedicated to determining or certifying nonclassicality of generated states for their potential future applications. [5–10]. Little attention, however, has been paid in multiphoton interference scenarios to the role of coherence distributed across the extent of the network. Yet, the inherent difference between local and global interferences suggests that their active control might offer unique insight into the interplay and convertibility of different forms of coherence within photonic networks.

In this Letter, we use coherent control over heralded single photons, spread over multiple nodes of a network, to demonstrate how their superposition state affects quantum interference patterns. We put forward correlation measures which certify the presence of two-particle quantum coherence across a linear optical network for probing local versus global coherence. Our implementation introduces a time-bin-multiplexing architecture with a compatible source of photons and configurable measurement for accessing various types of correlations. Identifying local and global correlations enables us to study contributions of the coherence properties of the source and distributed coherence properties of the network.

Controlling and observing two-photon interference.—We outline our approach in Fig. 1(a). The core of our

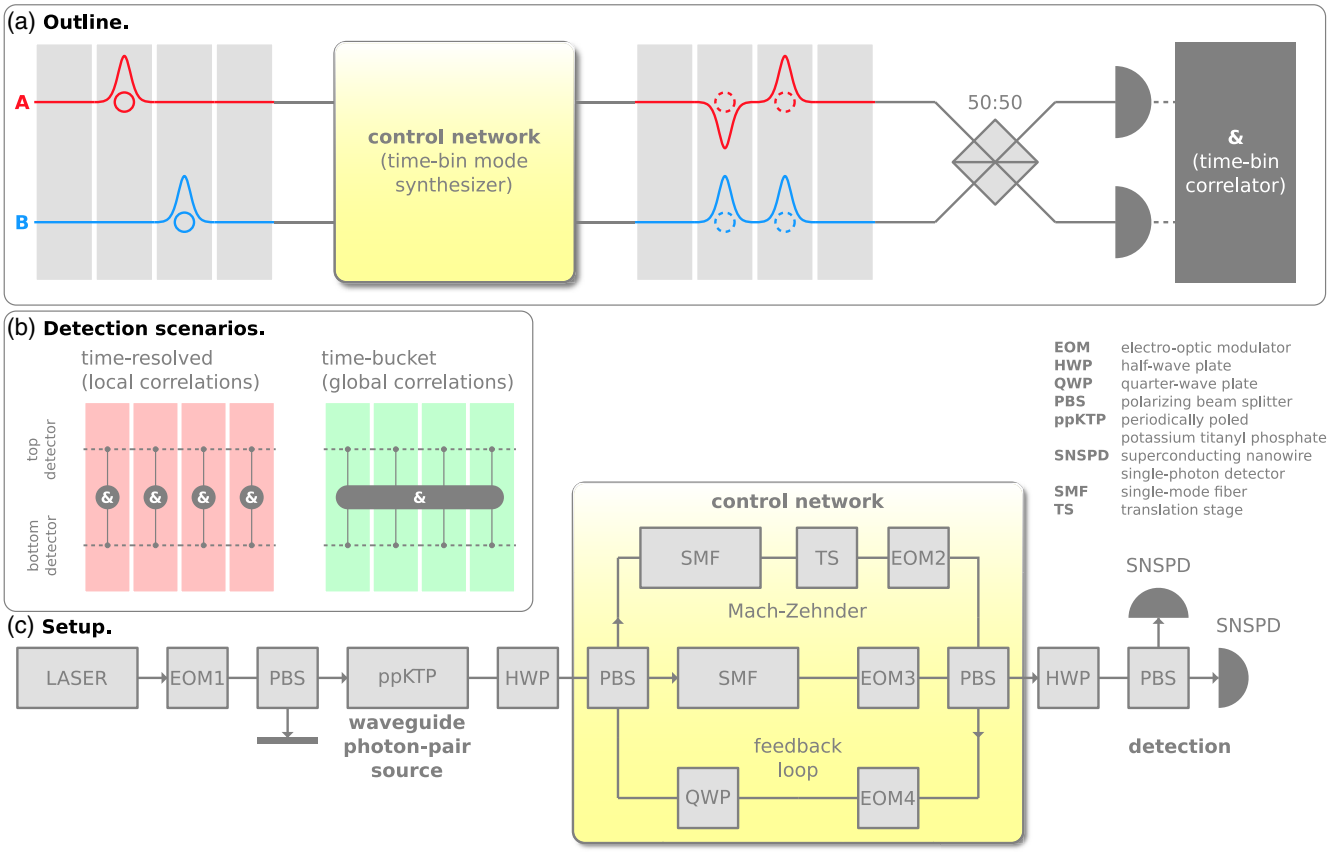

FIG. 1. (a) Two-photon interference protocol. Heralded single photons A and B are generated in different (time-bin) modes. Using a highly reconfigurable network, we synthesize arbitrary mode structures over which the photons are coherently distributed. In a subsequent HOM-type configuration, the two photons are superimposed, and correlations are measured. (b) Illustration of the two fundamentally different measures of correlation. Local correlations involve signals from the top and bottom detectors at the same time bin, while global correlations beyond HOM interferences access coincidences across multiple time bins. (c) Schematics of our setup. Our setup comprises state-of-the-art building blocks: a compatible photon source, a flexible control network (implemented as a time-multiplexed Mach-Zehnder interferometer with a feedback loop and deterministic in- and out-coupling), and a versatile detection stage.

system is a mode synthesizer which allows us to individually shape the time-bin mode structure of heralded single photons and, thereby, their interference characteristics. This is implemented using a linear photonic network, its crucial feature being reconfigurability. The realization of a mode synthesizer requires the ability to coherently manipulate selected degrees of freedom, such as polarization, frequency, or time-bin modes. Naturally, suitable single-photon sources and detectors must be available too.

Our experiments use a time-multiplexing fiber loop setup that provides a resource-efficient, scalable, stable, and flexible platform for the implementation of networks, and which has been used, among others, to realize quantum walks [21–24] and boson sampling [24–27]. Still, the dynamic operation of our network with multiple nonclassical single-photon states has not been shown to date, partly owing to the unavailability of a compatible source. The mode synthesis phase of our experiment is implemented by employing fast modulators and stable delay lines, resulting in each photon being coherently spread over multiple time bins. In the analysis phase, photons are brought to interference and measured with detectors capable of resolving individual time bins. In contrast to established HOM-type analysis procedures, coincidence events at the same time bin allow for assessing local correlations, and combined coincidences across multiple time bins are used for extracting global correlations [cf. Fig. 1(b)].

Ideal model for local and global correlations.—Using the standard quantum optics formalism [28], we can introduce a theoretical model that describes our system in the absence of imperfections. We label the initial photons as A and B, distributed in the control network over time bins as $\hat{A}^\dagger|\mathrm{vac}\rangle = \sum_\tau \alpha_\tau \hat{a}_\tau^\dagger|\mathrm{vac}\rangle$ and $\hat{B}^\dagger|\mathrm{vac}\rangle = \sum_\tau \beta_\tau \hat{b}_\tau^\dagger|\mathrm{vac}\rangle$, where $\hat{a}^\dagger$ and $\hat{b}^\dagger$ are bosonic creation operators for the modes under study (the index τ identifies the individual time-bin modes) and α and β are the corresponding probability amplitudes. A superposition of these photons on a 50:50 beam splitter results in output modes $(\hat{a}_\tau \pm \hat{b}_\tau)/\sqrt{2}$. The output correlations are measured with the top $(+)$ and bottom $(-)$ detector in Fig. 1, represented through photon-number operators $\hat{n}_{\pm,\tau}$. This yields the first-order correlation

$G^{(1)}_{\pm,\tau} = \langle \hat{n}_{\pm,\tau} \rangle = (|\alpha_\tau|^2 + |\beta_\tau|^2)/2$, giving the same values for both detectors, and the second-order cross-correlation

$$G^{(1,1)}_{\tau,\tau'} = \langle \hat{n}_{+,\tau} \hat{n}_{-,\tau'} \rangle = \frac{|\alpha_\tau \beta_{\tau'} - \alpha_{\tau'} \beta_\tau|^2}{4}. \quad (1)$$

To arrive at a refined notion of local and global correlations, we select a set of modes $\mathbb{S}$, potentially being a subset of all network modes. For convenience, we associate the vectors $\vec{\alpha} = [\alpha_\tau]_{\tau \in \mathbb{S}}$ and $\vec{\beta} = [\beta_\tau]_{\tau \in \mathbb{S}}$ with the photons A and B, respectively. This allows us to identify counts from a single detector, $G^{(1)}_{\pm} = \sum_{\tau \in \mathbb{S}} G^{(1)}_{\tau} = (\vec{\alpha}^\dagger \vec{\alpha} + \vec{\beta}^\dagger \vec{\beta})/2$.

Moreover, we arrive at compact formulas for correlation measures which characterize two-photon interference. For any selected set $\mathbb{S}$ of modes, we introduce local and global correlation measures via the sums

$$G^{(1,1)}_{\text{local}} = \sum_{\tau \in \mathbb{S}} G^{(1,1)}_{\tau,\tau} \quad \text{and} \quad G^{(1,1)}_{\text{global}} = \sum_{\tau,\tau' \in \mathbb{S}} G^{(1,1)}_{\tau,\tau'}, \quad (2)$$

respectively. By using Eq. (1), these correlations then obey

$$G^{(1,1)}_{\text{local}} = 0 \quad \text{and} \quad G^{(1,1)}_{\text{global}} = \frac{(\vec{\alpha}^\dagger \vec{\alpha})(\vec{\beta}^\dagger \vec{\beta}) - |\vec{\alpha}^\dagger \vec{\beta}|^2}{2}. \quad (3)$$

Expressions for experimentally relevant quantitites, such as normalized correlation functions, $g = G^{(1,1)}/[G^{(1)}_{+} G^{(1)}_{-}]$, and visibilities, $V = 1\text{–}2g$, can be readily obtained.

Beyond common HOM-type correlations, our approach offers a much deeper insight into the interplay of first- and second-order coherence properties of a network by evaluating the measured coincidences and interference visibilities. Since local correlations $G^{(1,1)}_{\text{local}}$ depend only on the source quality and imperfections of the network, the obtained visibilities relate to photon distinguishability at each time bin separately, exhibiting high visibility for high indistinguishability. In contrast, global correlations $G^{(1,1)}_{\text{global}}$ are additionally sensitive to the synthesized mode structure by correlating coincidences over multiple time bins.

Implementation.—At the core of our experimental setup lies a fiber-based unbalanced Mach-Zehnder interferometer with a feedback loop, as outlined in Fig. 1(c), that serves as a dynamically reconfigurable, time-multiplexing network [29]. The length difference of the single-mode fibers at the two interferometer arms sets the time-bin spacing (∼105 ns). A translation stage (TS) allows for a fine scanning of the time delays in the picosecond regime between the two interfering photons. The network contains fast electro-optic modulators (EOMs), capable of implementing controlled polarization rotations at any time bin. EOM2 and EOM3 ensure deterministic in- and outcoupling of the photons, whereas EOM4 allows synthetization of complex mode structures by programming appropriate switching patterns. A detailed description of our time-multiplexing scheme along with its specifications, and the details of our switching patterns, including the actual timings of the EOM operations for synthesizing the desired photon modes, are provided in the Supplemental Material (SM) [30].

In addition, we implement a new source via a type-II parametric down-conversion process in periodically poled potassium titanyl phosphate waveguide as an engineered source of heralded single photons with high spatial and spectral purity [31]. A picosecond pump laser at 775 nm and a bandwidth of ∼0.3 nm together with a 2.5 cm long waveguide generates relatively broad (∼2.7 ps) photon pulses at telecom wavelength. These picosecond photon pulses barely suffer from the difference in dispersive broadening in the fibers, thus maintaining good indistinguishability even after several round-trips through the network. To ensure that the two interfering photons are generated in desired time bins, we implement pulse picking on the pump laser using EOM1 and a polarization beam splitter (PBS). As a measure of the source quality, we obtain a visibility of the HOM coincidence count suppression of up to $V_0 = 0.801 \pm 0.067$, limited by the residual spectral distinguishability as well as higher photon-number terms in the heralded photon states. It is worth emphasizing that the nonunit visibility of our source is not an obstacle to accomplish our main objective of characterizing local and nonlocal coherence properties. To this goal, however, it is imperative to monitor the source visibility in each experiment that serves as a reference to exclude the source imperfections from the interference of the synthesized modes (see SM [30]).

Our detection scheme consists of two superconducting nanowire single-photon detectors with dead time and jitter well below the time-bin spacing, together with a PBS for separating the two polarizations, thus allowing both polarization and time-bin resolved measurements.

Results.—In Fig. 2, we present the results of our instructive two-photon interference analysis. In Figs. 2(a) and 2(b), the measured local and global coincidences are plotted against the delay introduced by the TS. Figure 2(a) corresponds to the case when the photons are distributed over two time bins such that their mode structures are expected to be orthogonal, described by two orthogonal vectors $\vec{\alpha}$ and $\vec{\beta}$, while correlations obtained for photons that are designed to have identical mode structures are given in Fig. 2(b). In both cases, the local correlations behave identically, and with visibilities significantly exceeding the classical threshold, certify local quantum features. Moreover, as expected from our simulations, the local visibilities resemble the corresponding source visibility. Global correlations that incorporate network effect via modal superposition, however, exhibit a remarkably different behavior depending on the global mode structure of the photons. For the first case [Fig. 2(a)], no interference is observed, certifying vanishing mode overlap, i.e.,

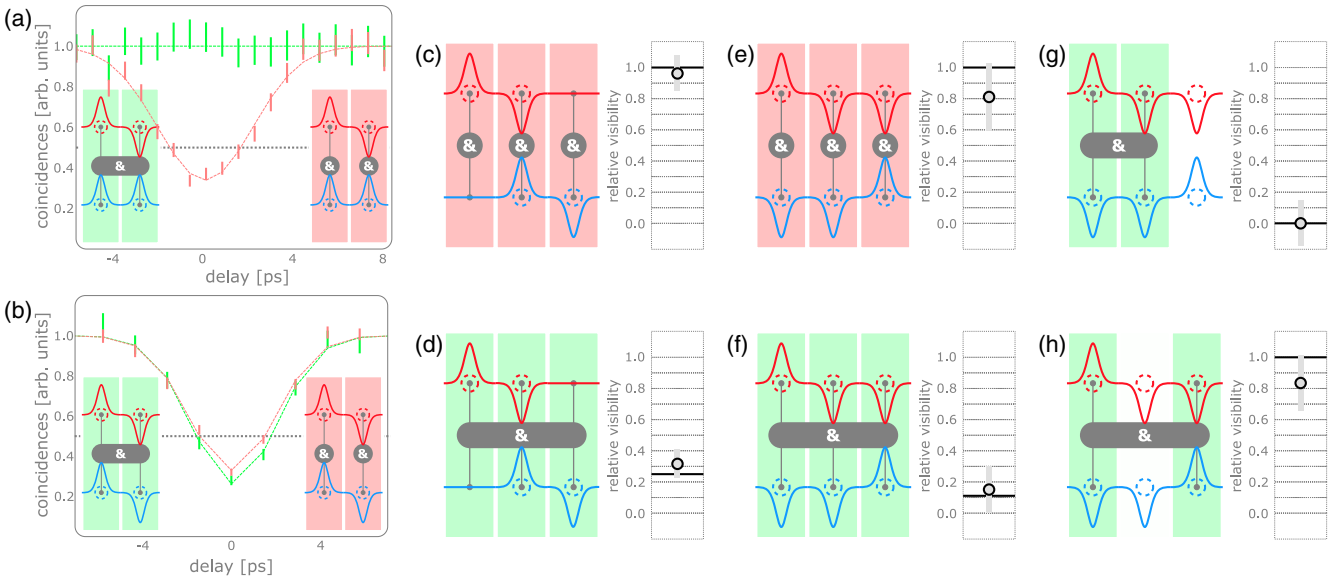

FIG. 2. Two-photon interference patterns for various synthesized mode structures. Plots (a) and (b) depict the interference via coincidences, where red and green data points indicate local and global detection scenarios (see insets). The curves indicate values obtained from a numerical model that includes imperfections, and the dotted line marks the quantum-classical boundary, certifying photon antibunching [32]. The characteristic HOM dip can be observed via local measurements, with visibilities close to the reference (i.e., source) value; see the SM for additional information [30]. Global coincidences correspond to the overlap of the synthesized photon modes, showing high two-photon coherence for parallel mode structures (b) and no interference for the orthogonal case (a). Plots (c)–(h) depict our results for different multimode interference scenarios. Assuming that V_0 is the dominant limiting factor on all cases, the visibilities (circles including error bars) are normalized by this value. The good agreement with the ideal model (thick solid line) justifies this assumption.

orthogonality of the photons' global mode structures $\hat{A}$ and $\hat{B}$. However, for the latter [Fig. 2(b)], the visibility of interference is roughly equal to those of local correlations, indicating an almost perfect mode overlap, thus validating that the photons' modes are identical.

The complete disappearance of the HOM dip in the orthogonal case in contrast to its maximum visibility in the parallel case (only limited by the source quality) highlights the near-perfect performance of the network and control over relative phases between the photons. Since the imperfection of the source can be factored out from the global visibilities, the markedly different behavior of global and local correlations allows for exact quantification of the nonlocal coherence, linked to the network and the local coherence dependent on the source. It is important to note that the certification of nonclassicality via a visibility $> 50\%$ is only relevant for source (i.e., local) coherence, which is successfully achieved at this point. Studying the global coherence shows that our nonclassical states can exhibit completely different two-photon interference behavior with visibilities which we can engineer to our will by designing appropriate global mode overlaps. For instance, the global visibility in Fig. 2(a) is zero although the states are clearly nonclassical single-photon states (as certified by local interference).

To explore the impact of coherent control for more complex mode structures, we synthesized various single-photon states involving three time bins, Figs. 2(c)–2(h). To factor out the effect of initial impurities, as argued above, we normalize all obtained visibilities by the corresponding reference (source) visibility and observe remarkably good agreement with the ideal model (thick solid lines). For additional details about the source visibility and the normalization, see the SM [30].

For Figs. 2(c) and 2(d), we considered photons spreading across two time bins but with a relative offset of one time bin. This is achieved through our unique control over the parameters $\vec{\alpha}$ and $\vec{\beta}$. This does not change the maximal local interference, Fig. 2(c). However, due to the reduced overlap between the photon states, our model predicts a reduced global visibility of 25% in Fig. 2(d) to which our experimental data agree with within the error margin. (Errors are obtained from standard statistical error analysis and error propagation.)

In Figs. 2(e)–2(h), we depict our results with photons in superposition of three modes. The preservation of the quality and the quantum nature of two-photon interference through the network is certified by local correlations shown in Fig. 2(e). Cross-correlations between all pairs of time bins, Fig. 2(f), are expected to yield a global visibility of $1/9 \approx 11\%$ for the generated pulse shapes, again being confirmed by our data. To reveal coherence between parts of the network, we consider correlations restricted to subsets of modes $\mathbb{S}$. For instance, when restricted to the

first two time bins, the two photons have orthogonal submode structures [Fig. 2(g)], thus yielding no visible interference. However, coincidences from time bins one and three [Fig. 2(h)], in which the photons have identical submode structure (up to a global phase), exhibit quantum coherence limited only by the photons' distinguishability [compare to Fig. 2(e)]. Additional details in the SM further support the excellent performance of our network [30].

Therefore, these results demonstrate how classical coherent control over the mode synthesizing network can be used to alter global quantum interference across several optical modes. Thus, by tailoring the time-bin-distributed shape of the input quantum light, we can generate and analyze the intricate details of coherent correlations of interfering quantum particles, despite our source not producing perfect single-photon states.

Summary and conclusion.—In summary, we established a generic scheme for jointly controlling and characterizing local and global coherence effects in the interference of multiple quantum particles. Using a time-multiplexed network for our on-demand mode synthesis, we determined interference visibilities to quantify the amount and kind of quantum coherence imprinted in the temporal distribution of two photons. Thereby, our experiment demonstrates an intricate interplay between classical mode interference and quantum coherence, and it serves as a testimony for how classical coherence can be used to govern quantum effects. Beyond purely assessing standard quantum HOM interference, our framework applies to any network architecture for the realization of a manifold of multimode coherence phenomena at will.

In the context of time multiplexing, our concepts can be intuitively related to extending standard HOM interference. However, this framework is applicable to any network implementation, e.g., spatial or frequency multiplexed, yielding a powerful tool for realizing and analyzing networkwide quantum coherence phenomena. The advantage of our characterization scheme is that instead of complex measurement settings and elaborate communication protocols between distant nodes of the network, it relies only on sufficient synchronization that allows individual parties to identify different runs, hence coincidence events. In addition to the high-performance network and intricate detection part, a compatible source of single photon has been implemented, requiring a setup overhaul and optimization to reliably operate in the single-photon regime instead of using bright coherent light.

Our results certify an unprecedented level of control that extends over multiple modes and which enables us to manipulate quantumness not only locally, but globally. This includes engineering interference between arbitrarily selected parts of the full system. Our coherent control renders it possible to purposefully alter our system toward any desired interference for studying the rich landscape of quantum superpositions of particles. Furthermore, our network has no fundamental restrictions regarding future increments of the number of modes and photons, thus paving the route for photonic quantum information science, such as quantum simulators [33] and remote state preparation protocols [34], which exploit different forms of multiphoton quantum interference phenomena.

The Integrated Quantum Optics group acknowledges financial support through the European Commission through the ERC project QuPoPCoRN (Grant No. 725366) and the Gottfried Wilhelm Leibniz-Preis (Grant No. SI1115/3-1). A. G. and I. J. received financial support by the Czech Science foundation (GAČR) Project No. 17-00844S and by RVO 14000. I. J. acknowledges funding from the project "Centre for Advanced Applied Sciences," Registry No. CZ.02.1.01/0.0/0.0/16_019/0000778, supported by the Operational Programme Research, Development and Education, co-financed by the European Structural and Investment Funds and the state budget of the Czech Republic, and A. G. by the National Research Development and Innovation Office of Hungary under Project No. K124351.

*syamsundar.de@upb.de

[1] R. Loudon, *The Quantum Theory of Light* (Oxford University Press, Oxford, 1973).
[2] O. Donati, G. P. Missiroli, and G. Pozzi, An experiment on electron interference, Am. J. Phys. **41**, 639 (1973).
[3] C. K. Hong, Z. Y. Ou, and L. Mandel, Measurement of Subpicosecond Time Intervals between Two Photons by Interference, Phys. Rev. Lett. **59**, 2044 (1987).
[4] J.-W. Pan, Z.-B. Chen, C.-Y. Lu, H. Weinfurter, A. Zeilinger, and M Żukowski, Multiphoton entanglement and interferometry, Rev. Mod. Phys. **84**, 777 (2012).
[5] A. Kuzmich, D. Branning, L. Mandel, and I. A. Walmsley, Multiphoton interference effects at a beamsplitter, J. Mod. Opt. **45**, 2233 (1998).
[6] B. J. Metcalf *et al.*, Multiphoton quantum interference in a multiport integrated photonic device, Nat. Commun. **4**, 1356 (2013).
[7] M. Tillmann, S.-H. Tan, S. E. Stoeckl, B. C. Sanders, H. de Guise, R. Heilmann, S. Nolte, A. Szameit, and P. Walther, Generalized Multiphoton Quantum Interference, Phys. Rev. X **5**, 041015 (2015).
[8] L. Rigovacca, C. Di Franco, B. J. Metcalf, I. A. Walmsley, and M. S. Kim, Nonclassicality Criteria in Multiport Interferometry, Phys. Rev. Lett. **117**, 213602 (2016).
[9] S. Agne, T. Kauten, J. Jin, E. Meyer-Scott, J. Z. Salvail, D. R. Hamel, K. J. Resch, G. Weihs, and T. Jennewein, Observation of Genuine Three-Photon Interference, Phys. Rev. Lett. **118**, 153602 (2017).
[10] Á. Navarrete, W. Wang, F. Xu, and M. Curty, Characterizing multi-photon quantum interference with practical light sources and threshold single-photon detectors, New J. Phys. **20**, 043018 (2018).

[11] H. M. Wiseman and G. J. Milburm, *Quantum Measurement and Control* (Cambridge University Press, Cambridge, England, 2010).
[12] A. M. Childs, D. Gosset, and Z. Webb, Universal computation by multiparticle quantum walk, Science **339**, 791 (2013).
[13] E. Knill, R. Laflamme, and G. J. Milburn, A scheme for efficient quantum computation with linear optics, Nature (London) **409**, 46 (2001).
[14] R. Raussendorf and H. J. Briegel, A One-Way Computer, Phys. Rev. Lett. **86**, 5188 (2001).
[15] J. L. O'Brien, A. Furusawa, and J. Vučković, Photonic quantum technologies, Nat. Photonics **3**, 687 (2009).
[16] Y. H. Shih and C. O. Alley, New Type of Einstein-Podolsky-Rosen-Bohm Experiment Using Pairs of Light Quanta Produced by Optical Parametric Down Conversion, Phys. Rev. Lett. **61**, 2921 (1988).
[17] P. G. Kwiat, A. M. Steinberg, and R. Y. Chiao, Observation of a quantum eraser: A revival of coherence in a two-photon interference experiment, Phys. Rev. A **45**, 7729 (1992).
[18] T. Legero, T. Wilk, M. Hennrich, G. Rempe, and A. Kuhn, Quantum Beat of Two Single Photons, Phys. Rev. Lett. **93**, 070503 (2004).
[19] A. J. Menssen, A. E. Jones, B. J. Metcalf, M. C. Tichy, S. Barz, W. S. Kolthammer, and I. A. Walmsley, Distinguishability and Many-Particle Interference, Phys. Rev. Lett. **118**, 153603 (2017).
[20] M. Rezai, J. Sperling, and I. Gerhardt, What can single photons do what lasers cannot do?, Quantum Sci. Technol. **4**, 045008 (2019).
[21] Y. Aharonov, L. Davidovich, and N. Zagury, Quantum random walks, Phys. Rev. A **48**, 1687 (1993).
[22] A. Schreiber, K. N. Cassemiro, V. Potoček, A. Gábris, P. J. Mosley, E. Andersson, I. Jex, and C. Silberhorn, Photons Walking the Line: A Quantum Walk with Adjustable Coin Operations, Phys. Rev. Lett. **104**, 050502 (2010).
[23] T. Nitsche, S. Barkhofen, R. Kruse, L. Sansoni, M. Štefaňák, A. Gábris, V. Potoček, T. Kiss, I. Jex, and C. Silberhorn, Probing measurement-induced effects in quantum walks via recurrence, Sci. Adv. **4**, eaar6444 (2018).
[24] S. Aaronson and A. Arkhipov, The computational complexity of linear optics, in *Proceedings of the Forty-Third Annual ACM Symposium on Theory of Computing, (ACM), STOC 11* (Association for Computing Machinery, New York, 2011), pp. 333–342.
[25] K. R. Motes, A. Gilchrist, J. P. Dowling, and P. P. Rohde, Scalable Boson Sampling with Time-Bin Encoding Using a Loop-Based Architecture, Phys. Rev. Lett. **113**, 120501 (2014).
[26] Y. He, X. Ding, Z.-E. Su, H.-L. Huang, J. Qin *et al.*, Time-Bin-Encoded Boson Sampling with a Single-Photon Device, Phys. Rev. Lett. **118**, 190501 (2017).
[27] M. Walschaers, Signatures of many-particle interference, J. Phys. B **53**, 043001 (2020).
[28] L. Mandel and E. Wolf, *Optical Coherence and Quantum Optics* (Cambridge University Press, Cambridge, England, 1995).
[29] T. Nitsche, F. Elster, J. Novotný, A. Gábris, I. Jex, S. Barkhofen, and C. Silberhorn, Quantum walks with dynamical control: Graph engineering, initial state preparation and state transfer, New. J. Phys. **18**, 063017 (2016).
[30] See Supplemental Material at http://link.aps.org/supplemental/10.1103/PhysRevLett.125.213604, which includes Refs. [22,29], for details on the experiment and additional results.
[31] G. Harder, V. Ansari, B. Brecht, T. Dirmeier, C. Marquardt, and C. Silberhorn, An optimized photon pair source for quantum circuits, Opt. Express **21**, 13975 (2013).
[32] H. J. Kimble, M. Dagenais, and L. Mandel, Photon Antibunching in Resonance Fluorescence, Phys. Rev. Lett. **39**, 691 (1977).
[33] A. Aspuru-Guzik and P. Walther, Photonic quantum simulators, Nat. Phys. **8**, 285 (2012).
[34] C. H. Bennett, P. Hayden, D. W. Leung, P. W. Shor, and A. Winter, Remote preparation of quantum states, IEEE Trans. Inf. Theory **51**, 56 (2005).